ACS OMEGA

Open Access

http://pubs.acs.org/journal/acsodf

Article

Shuganning Injection Suppresses Apoptosis for Protecting Against Cantharidin-Induced Liver Injury by Network Pharmacology and Experiment Validation

Xiaotong Duan, Jingwen Ao, Ming Yu, Sali Li, Xiaofei Li,* and Jianyong Zhang*

Cite This: *ACS Omega* 2024, 9, 13692−13703

Read Online

ACCESS | Metrics & More | Article Recommendations

ABSTRACT: Cantharidin (CTD) is a compound of mylabris with antitumor activity, and CTD can potentially cause toxicity, especially hepatotoxicity. The classical Traditional Chinese Medicine prescription Shuganning injection (SGNI) exerts notable anti-inflammatory and hepatoprotective effects. However, the protective property and mechanism of SGNI against CTD-induced liver injury (CTD-DILI) have not yet been elucidated. To investigate the effective compounds, potential targets, and molecular mechanism of SGNI against CTD-DILI, network pharmacology combined with experiments were performed. This study found that SGNI could act with 62 core therapeutic targets, regulate multiple biological processes such as apoptosis, and oxidative stress, and influence apoptotic and p53 signaling pathways to treat CTD-DILI. Subsequently, HepaRG cell experiments demonstrated that SGNI pretreatment significantly increased the levels of GSH-Px and SOD, inhibiting the apoptosis induced by CTD. In vivo, according to H&E staining, SGNI can reduce the degeneration of hepatocytes and cytoplasmic vacuolation in mice exposed to CTD. Western blot analysis results indicated that SGNI pretreatment significantly suppressed the expressions of Caspase-3 and Bax while increasing the expression of Bcl-2. In conclusion, SGNI acted as a protective agent against CTD-DILI by inhibiting apoptosis.

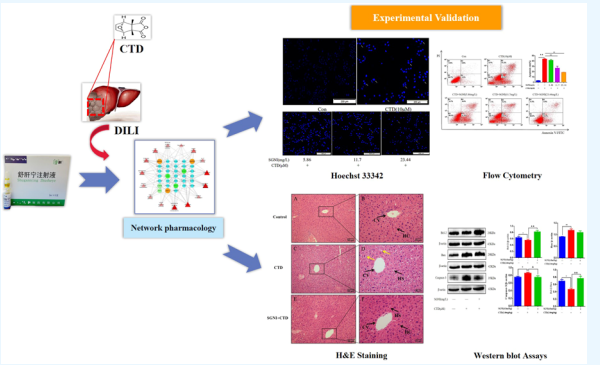

1. INTRODUCTION

Cantharidin (CTD), a major compound secreted by *Mylabris* species,[1] has effective antitumor activity and has been used to treat a variety of cancers, such as liver, lung,[2,3] and pancreatic cancers.[4,5] However, the hepatotoxicity of CTD limits its clinical application.[6] In a previous study, CTD inhibited endoplasmic reticulum stress and induced autophagy and apoptosis in LO2 human hepatocytes.[7] CTD can also induce liver injury by activating inflammatory responses and oxidative stress.[8,9] No specific treatment currently exists for CTD-induced liver injury (CTD-DILI), whereas Traditional Chinese Medicine (TCM) has a strong potential in treating CTD hepatotoxicity due to its multitarget and multi-pathway characteristics.

TCM has extensive experience and unique advantages in the treatment of drug-induced liver injury. Shuganning injection (SGNI), developed from Yinchenhao Decoction of classical Chinese prescription, which has been commonly used in Chinese clinical practice for the prevention and treatment of hepatopathy for thousands of years.[10] It was a traditional Chinese material standardized clinical product prepared from the extracts of *Artemisia scoparia* Waldst & Kitam. (YC), *Gardenia jasminoides* J. Ellis (ZZ), *Scutellaria baicalensis* Georgi (HQG), *Isatis tinctoria* L. (BLG), and *Gardenia lucida* Roxb. (LZ) (the plant name has been checked with http://www.theplantlist.org on October 10, 2022) as in Table 1.[11,12] Several clinical studies have reported that SGNI has a hepatoprotective effect and can significantly improve liver function, warranting clinical application.[13] Clinical studies have demonstrated that SGNI combined with tiopronin can treat drug-induced liver disease, and animal experiments have demonstrated that SGNI has significant preventive and therapeutic effects on cisplatin-induced liver injury in mice.[14−16] ZZ, HQG, and LZ in SGNI were reported to protect the liver from acetaminophen (APAP) through anti-inflammatory effects and oxidative stress inhibition.[17] However, its major effective compounds, potential targets, and molecular mechanism remain unclear.

Network pharmacology can predict the bioactive compounds, multiple targets, and potential pathways of TCM through system biology, multivariate pharmacology, and molecular

Received: October 12, 2023
Revised: January 12, 2024
Accepted: January 16, 2024
Published: March 12, 2024

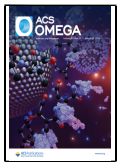

Table 1. Components of SGNI Injection[a]

scientific name	herbal name	Chinese name	family	amount (g/L)
Artemisia scoparia Waldst and Kitam.	Artemisiae Scopariae Herba	Yin Chen (YC)	Compositae	4
Gardenia jasminoides J. Ellis	Gardeniae Fructus	Zhi Zi (ZZ)	Rubiaceae	3
Scutellaria baicalensis Ceorgi	Baicalin	Huang Qingan (HQG)	Lamiaceae	22
Isatis tinctoria L.	Isatidis Radix	Ban Langen (BLG)	Brassicaceae	5
Gardenia lucida Roxb.	Gardenia	Ling Zhi (LZ)	Gardenia	3.5

[a]1000 mL Shuganning Injection (SGNI) is extracted from Yinchen (4 g), Zhizhi (3 g), Huang Qingan (22 g), Ban Langen (5 g), and Lingzhi (3.5 g).

network analysis. Tang et al. identified 37 potential targets related to AR in Mahuang Fuzi Xixin decoction through network pharmacology and predicted that four were closely associated with anti-inflammatory effects.[18] In this study, network pharmacology with vitro cell experimental verification was applied to construct a reliable systematic network to predict and verify the major effective compounds, potential targets, and molecular mechanisms of SGNI for CTD-DILI. Moreover, an experimental cell model of CTD-DILI was then established to detect the role of SGNI in CTD-induced apoptosis.

2. RESULTS

2.1. Network Construction. *2.1.1. Components and Targets of Herbs in the SGNI.* From TCMSP, 308 active SGNI compounds were found. Furthermore, active targets were screened using TCMSP and Targetnet databases. After integrating UniProt database entries and eliminating duplicates, 438 active targets were obtained (Figure 1A).

2.1.2. Overlapping Targets between SGNI and CTD-DILI. After combining the filtering target results of GeneCards, CTD, and Digsee databases and eliminating the duplicates, 93 CTD-DILI targets were obtained (Figure 1B). The 93 CTD-DILI targets and 438 active SGNI targets were intersected, thus obtaining 62 SGNI-DILI core targets (Figure 1C).

2.1.3. PPI Network and Core Targets. Based on the 62 core targets, a PPI network was established by importing the gene ID of the core targets to the STRING. The color and size of the nodes reflected their degree value, with larger and darker nodes indicating a higher degree value. The network also indicated that HSP90AA1, AKT1, MAPK1, CASP3, and JUN were the top five targets with the highest degree. The results suggest that these SGNI targets have a substantial effect on CTD-DILI (Figure 1D).

2.1.4. GO Functional Enrichment and KEGG Pathway Analysis. The GO enrichment analysis of 62 core targets was performed in the DAVID 6.8 database. The GO analysis demonstrated that 209 biological processes (BP), 22 cell components (CC), and 57 molecular functions (MF) were found in the DAVID database (Figure 1E). BP mainly involves the apoptotic process, cell proliferation, and gene expression, whereas CC mainly involves a macromolecular complex, nucleoplasm, and cytoplasm. MF mainly involves enzyme binding, identical protein binding, and oxidoreductase activity. The results indicated that the mechanisms of SGNI against CTD-DILI were associated with the apoptotic process, oxidative stress, cell proliferation, and cell cycle.

To predict the potential signaling pathways of SGNI protection against DILI, we performed a KEGG enrichment analysis on 62 core targets. A total of 66 pathways were observed to be significantly associated with the input set of genes ($P < 0.01$), and the top 15 pathways were shown in bubble charts (Figure 2A), including the apoptosis signaling pathway, the AGE-RAGE signaling pathway in diabetic complications, the estrogen signaling pathway, the p53 signaling pathway, the sphingolipid signaling pathway, the IL-17 signaling pathway, the steroid hormone biosynthesis, and the TNF signaling pathway. Furthermore, to elucidate the interrelationships of targets and the top 15 pathways, we constructed a Target-Pathway network (T-P) containing 250 nodes and 125 edges (Figure 2B). The essential genes were mainly distributed in the apoptosis signaling pathway (Figure 2C), indicating that SGNI may ameliorate CTD-related symptoms through the apoptosis signaling pathway.

2.2. Effect of SGNI on Cell Viability of HepaRG Cells Injured by CTD. The relative cell viability decreased after treatment of CTD (0, 1.25, 2.5, 5, 10, and 20 μM) in a dose-dependent manner with an IC_{50} value of 13.16 μM. At concentrations of 5.86, 11.7, 23.44, and 46.88 mg/L, SGNI did not damage the viability of HepaRG cells; however, 93.75 mg/L SGNI slightly decreased cell viability. Therefore, 5.86, 11.7, 23.44, and 46.88 mg/L SGNI were selected for subsequent experiments ($p < 0.01$) (Table 2). By contrast, SGNI pretreatment at varying concentrations of 11.7, 23.44, and 46.88 mg/L inhibited CTD-induced cell death compared with the CTD group ($p < 0.01$) (Figure 3). The CTD-induced cytotoxicity on HepaRG cells was significantly reversed through SGNI treatment, suggesting that SGNI may protect against CTD-DILI in HepaRG cells.

2.3. Effect of SGNI on the Levels of Liver Function Enzyme of HepaRG Cells Injured by CTD. Compared with the control group, the levels of alanine aminotransferase (ALT), aspartate aminotransferase (AST), and lactate dehydrogenase (LDH) significantly increased ($p < 0.01$), suggesting that CTD caused cell injury. Meanwhile, high levels of ALT and AST induced by CTD were markedly reversed by SGNI pretreatment (5.86, 11.7, and 23.44 mg/L) in a dose-dependent manner ($p < 0.01$) (Figure 4). These results demonstrated that SGNI treatment alleviated the CTD-DILI of HepaRG cells.

2.4. Effects of SGNI on Oxidative Stress Activity in the Supernatant of HepaRG Cells Injured by CTD. The MDA content in HepaRG cells was markedly increased in the CTD group compared to that in the control group ($p < 0.01$). The malondialdehyde (MDA) content in the 11.7 mg/L (4.24 ± 0.12 nmol/mg) or 23.44 mg/L (3.28 ± 0.16 nmol/mg) SGNI-treated groups significantly decreased than those in the CTD group ($p < 0.01$). The activities of glutathione peroxidase (GSH-Px) (34.37 ± 2.69 μmol/g) and superoxide dismutase (SOD) (30.5 ± 1.52 μmol/g) in the CTD groups were lower than those in the control group ($p < 0.01$). Conversely, the activities of GSH-Px and SOD in the SGNI-treated groups significantly increased compared to those in the CTD group (Figure 5). These results indicate that SGNI can improve CTD-DILI by stimulating the production of antioxidant enzymes and inhibiting peroxidation.

2.5. Nuclear Morphological Observation. Compared with the control cells, the cells treated with CTD (10 μM) for 12 h exhibited an apoptotic morphology, characterized by cell

https://doi.org/10.1021/acsomega.3c07981
ACS Omega 2024, 9, 13692−13703

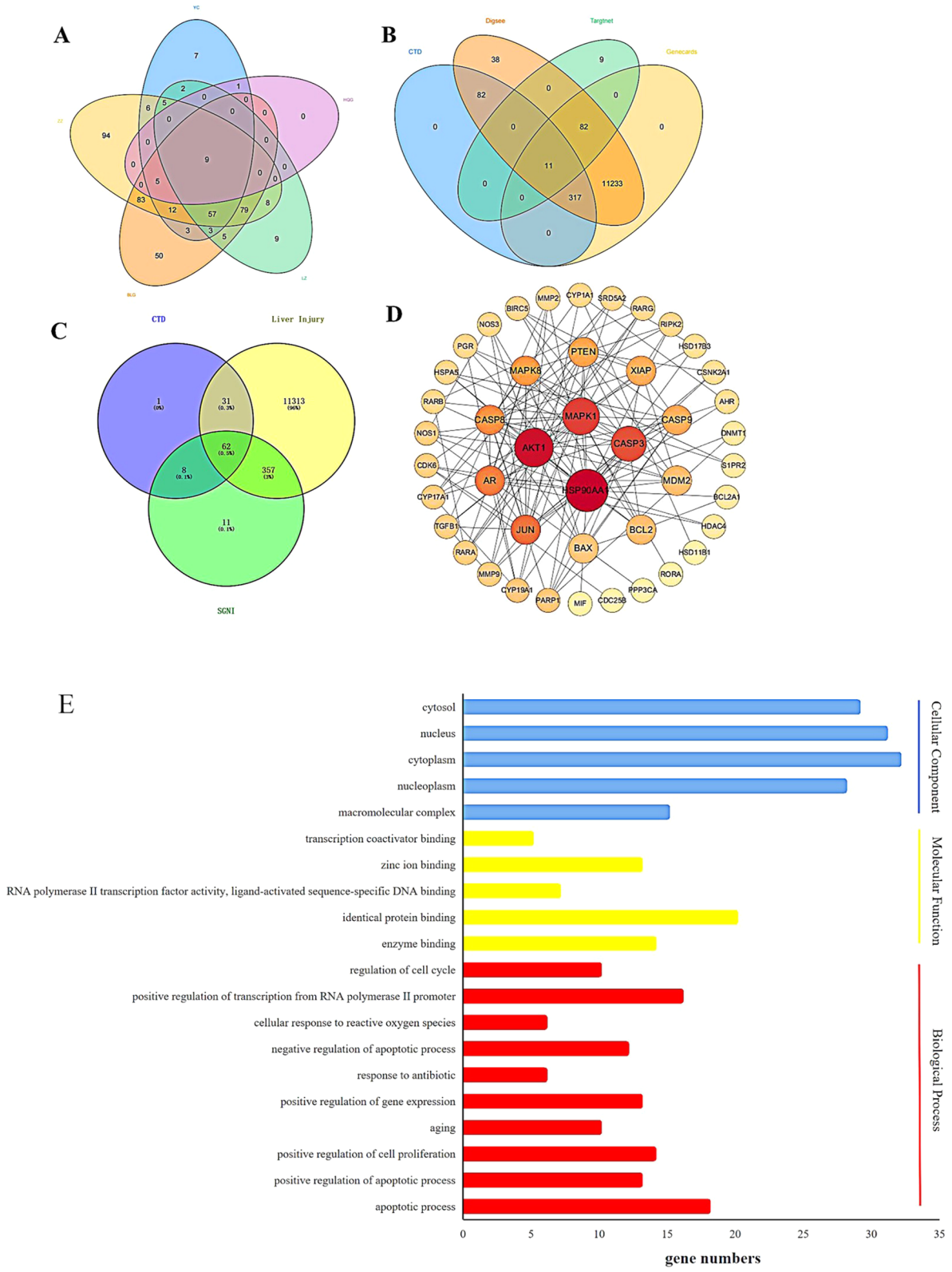

Figure 1. Network analysis of SGNI target genes and CTD differentially expressed genes. (A) Mapping of the key targets of five groups of herbs in SGNI. (B) Venn diagram of genes associated with hepatotoxicity. (C) Venn diagram of SGNI target genes and CTD-induced liver injury differentially expressed genes. (D) Protein−protein interaction (PPI) network of the quercetin target genes. A bigger node size meant a higher value. With the increasing degree value, the node color becomes darker. (E) GO enrichment analysis of SGNI targets in treating CTD. The horizontal axis of the BP, CC, and MF columns represents the number of genes enriched in each item.

nuclei pyknosis and asymmetric chromatin condensation. When HepaRG cells were cotreated with CTD (10 μM) and SGNI (5.86, 11.7, and 23.44 mg/L), the fluorescence intensity decreased gradually, and the number of apoptotic cells

https://doi.org/10.1021/acsomega.3c07981
ACS Omega 2024, 9, 13692−13703

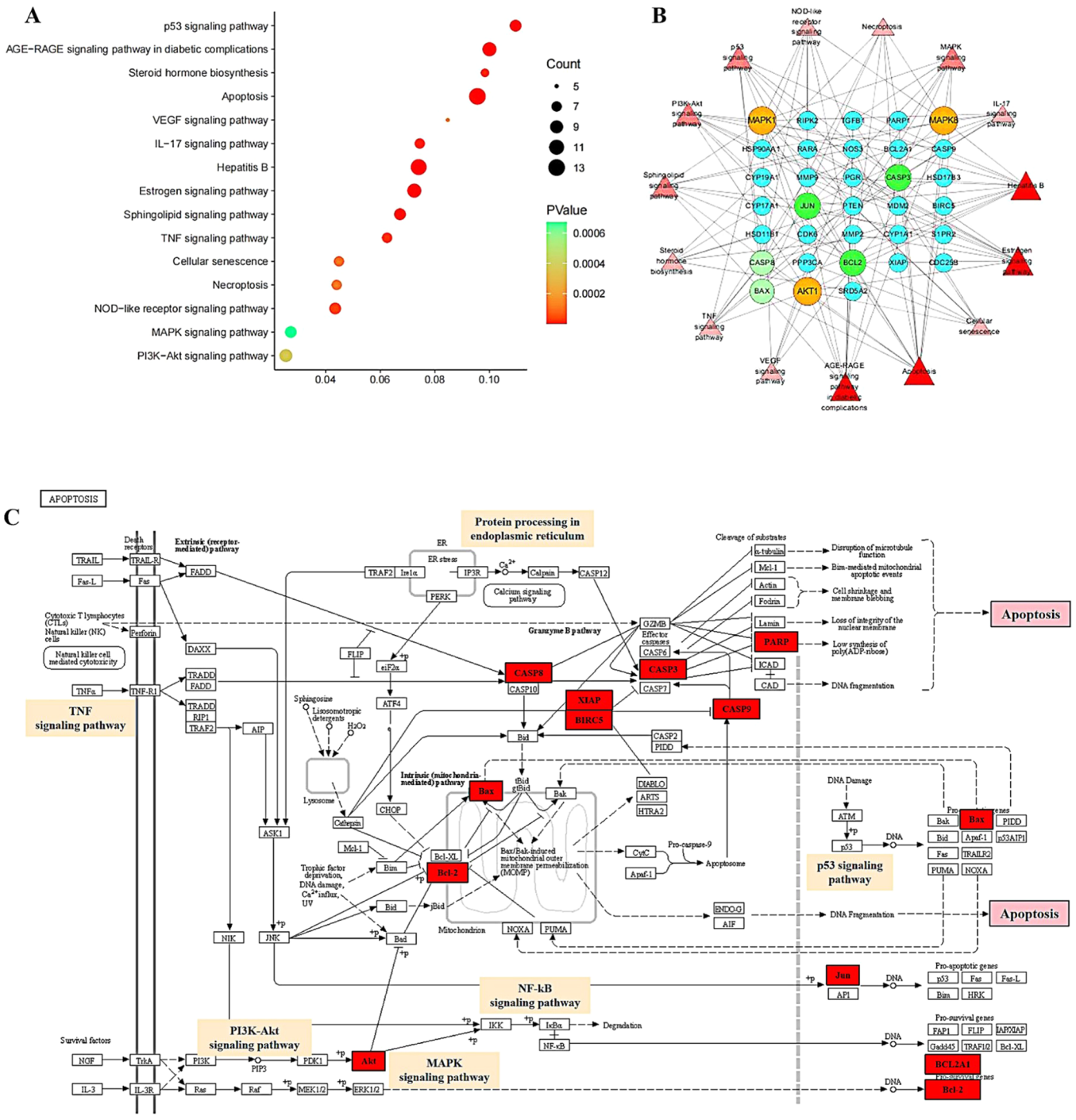

Figure 2. KEGG enrichment analysis of the SGNI targets. (A) KEGG annotation of target genes. The number of genes enriched in each KEGG term is shown as the circle size, and the *p*-value is shown as different colors. (B) KEGG relational regulatory network. This network shows the relationship between the enriched 15 pathways and 33 genes, and the size of the graph shows the number of pathways or genes connected. (C) Important genes are mainly distributed in the apoptosis signaling pathway. Arrows represent the activation effect; T-arrows represent the inhibition effect. The red nodes are the intersection genes.

decreased ($p < 0.01$) (Figure 6). These results indicated that characteristic morphological changes accompanied the CTD-induced apoptosis of HepaRG cells and that SGNI alleviated CTD-induced cell apoptosis.

2.6. Protective Effects of SGNI against CTD-Induced Apoptosis. We assessed the effect of SGNI in various concentrations (5.86, 11.7, and 23.44 mg/L) on CTD (10 μM)-induced apoptosis. The rate of early cell apoptosis was represented in the B4 region, whereas the rate of late cell apoptosis was represented in the B2 region. After 12 h of incubation with CTD (10 μM), the cell apoptosis rate significantly increased relative to that of the control group. With SGNI pretreatment for 12 h, the rate of cell apoptosis decreased relative to the CTD stimulation group, and the cells treated with 5.86, 11.7, and 23.44 mg/L of SGNI exhibited significant protection effects ($p < 0.01$) (Figure 7). Flow cytometry revealed that SGNI potently inhibited CTD-induced

https://doi.org/10.1021/acsomega.3c07981
ACS Omega 2024, 9, 13692−13703

Table 2. Effects of CTD and SGNI on HepaRG Cell Viability

CTD (μM)	cell viability (%)	SGNI (mg/L)	cell viability (%)
0	100.00 ± 0.00	0	100.00 ± 0.00
1.25	94.72 ± 3.03	5.86	98.47 ± 3.07
2.5	88.77 ± 3.46*	11.7	96.95 ± 5.77
5	75.62 ± 3.99**	23.44	92.88 ± 1.45
10	66.49 ± 0.48**	46.88	93.17 ± 1.36
20	31.75 ± 4.86**	93.75	85.94 ± 2.16*

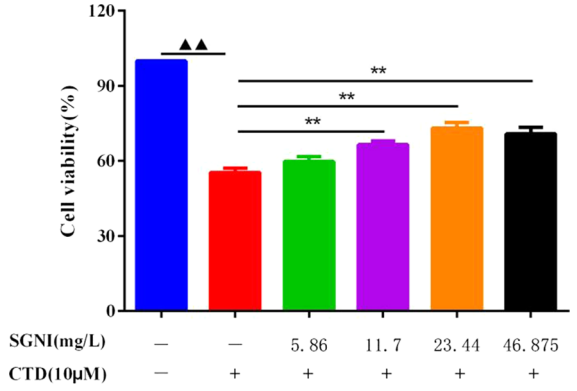

Figure 3. Protective Effect of SGNI on CTD-DILI in HepaRG cells. Data are expressed as mean ± SD (n = 3). ▲▲p < 0.01 compared with control, **p < 0.01 compared with CTD.

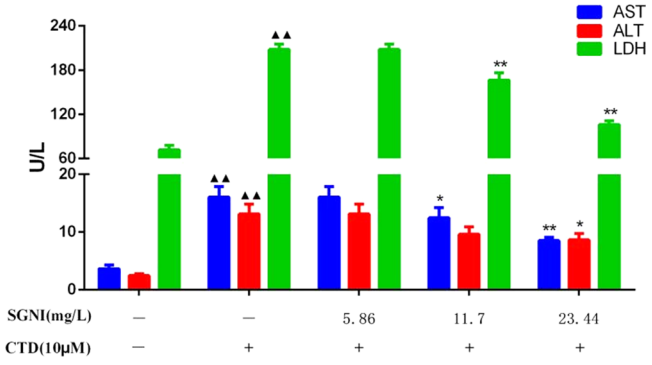

Figure 4. Effect of SGNI on the activities of AST, ALT and LDH in CTD-induced. Data are expressed as mean ± SD (n = 3). ▲▲p < 0.01 compared with control, *p < 0.05, **p < 0.01 compared with CTD.

apoptosis and had a potential antiapoptotic effect on HepaRG cells.

2.7. Evaluation of mRNA Levels of Apoptosis Genes. To further validate the apoptosis mechanism in HepaRG cells in response to SGNI treatment, we examined the mRNA expression of Bcl-2, Bax, and Caspase-3. The results demonstrated that CTD enhanced the mRNA levels of Bax and Caspase-3 but reduced the Bcl-2 expression in HepaRG cells relative to the control groups (p < 0.01). Compared with CTD (10 μM), the expression level of Bax and Caspase-3 in the SGNI (23.44 mg/L) group decreased, whereas the Bcl-2 expression level increased. These results suggested that SGNI could reduce apoptosis in CTD-induced HepaRG cells with the down-regulation of Bax and Caspase-3 mRNA and protein expression levels and the up-regulation of Bcl-2 mRNA expression levels (p < 0.01) (Figure 8).

2.8. Evaluation of Cellular Apoptosis Protein Expression Levels. Consistent with prior studies, Western blot analysis demonstrated that the protein expressions of Bax and Caspase-3 increased, whereas Bcl-2 expression decreased in CTD-stimulated HepaRG cells relative to that in the control cells. Furthermore, SGNI remarkably inhibited CTD-induced Bax and Caspase-3 overexpression, whereas it enhanced Bcl-2 expression in a dose-dependent manner at 12 h (Figure 9). These collective data suggest that SGNI may have an antiapoptotic effect on CTD-stimulated HepaRG cells by suppressing Caspase-3 expression and increasing Bcl-2/Bax expression.

2.9. SGNI Pretreatment Exerted a Hepatoprotective Effect in CTD-Induced Mice. The mice and liver were weighed, and the liver weight/body weight ratio (mg/g) was calculated. The liver weight/body weight ratio of the CTD group mice was significantly increased compared with the control group, and the liver weight/body weight ratio of the SGNI pretreatment group was significantly decreased compared with the CTD group (Figure 10A). As displayed in Figure 10B–D, mice treated with CTD for 7 consecutive days manifested severe liver damage, which was demonstrated by a significant elevation of ALT, AST, and LDH levels in comparison to the control. SGNI pretreatment significantly reduced the serum ALT, AST, and LDH levels, respectively, compared to the CTD-induced liver injury mice (p < 0.05).

In order to further analyze the effects of SGNI, we performed hematoxylin and eosin (H&E) staining to examine the histology of the livers. H&E staining revealed that the liver of mice in the control group (Figure 11A,B) had normal hepatic ultrastructure and no steatosis. By contrast, the liver of mice in the CTD group (Figure 11C,D) had disorganized cords, deformed and compressed hepatocytes, and cytoplasmic accumulation of lipid droplets with varied size, number, and shape. However, these histological changes were dramatically lightened by SGNI pretreatment (Figure 11E,F), most of the hepatocytes had a normal ultrastructure, intact cell membranes, and less lipid droplet accumulation.

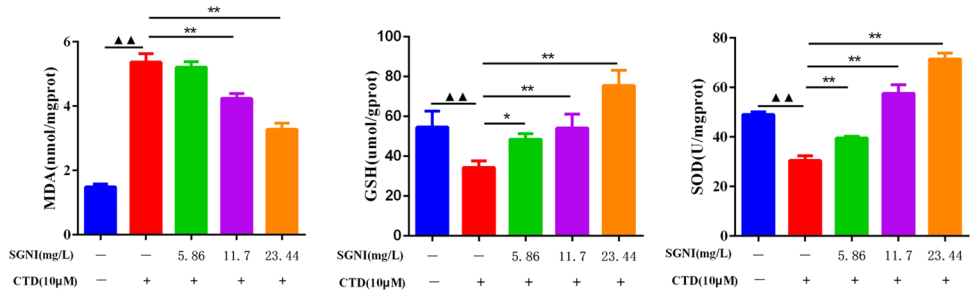

Figure 5. Effect of SGNI on oxidative stress in the HepaRG cells of CTD-induced. Data are expressed as mean ± SD (n = 3). ▲p < 0.05, ▲▲p < 0.01 compared with control, and * p < 0.05, **p < 0.01 compared with CTD.

https://doi.org/10.1021/acsomega.3c07981
ACS Omega 2024, 9, 13692−13703

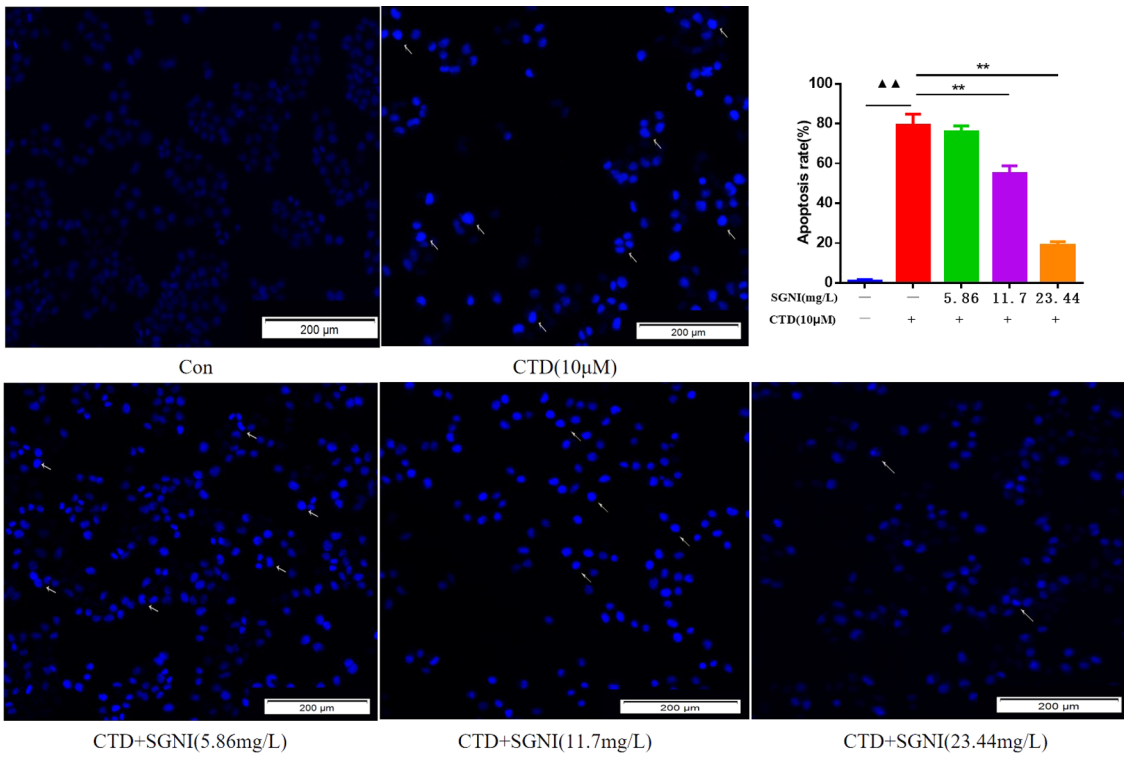

Figure 6. Morphological changes of the HepaRG cell nucleus were detected by Hoechst 33342. Data are expressed as mean ± SD ($n = 3$). ▲▲$p < 0.01$ compared with control, **$p < 0.01$ compared with CTD.

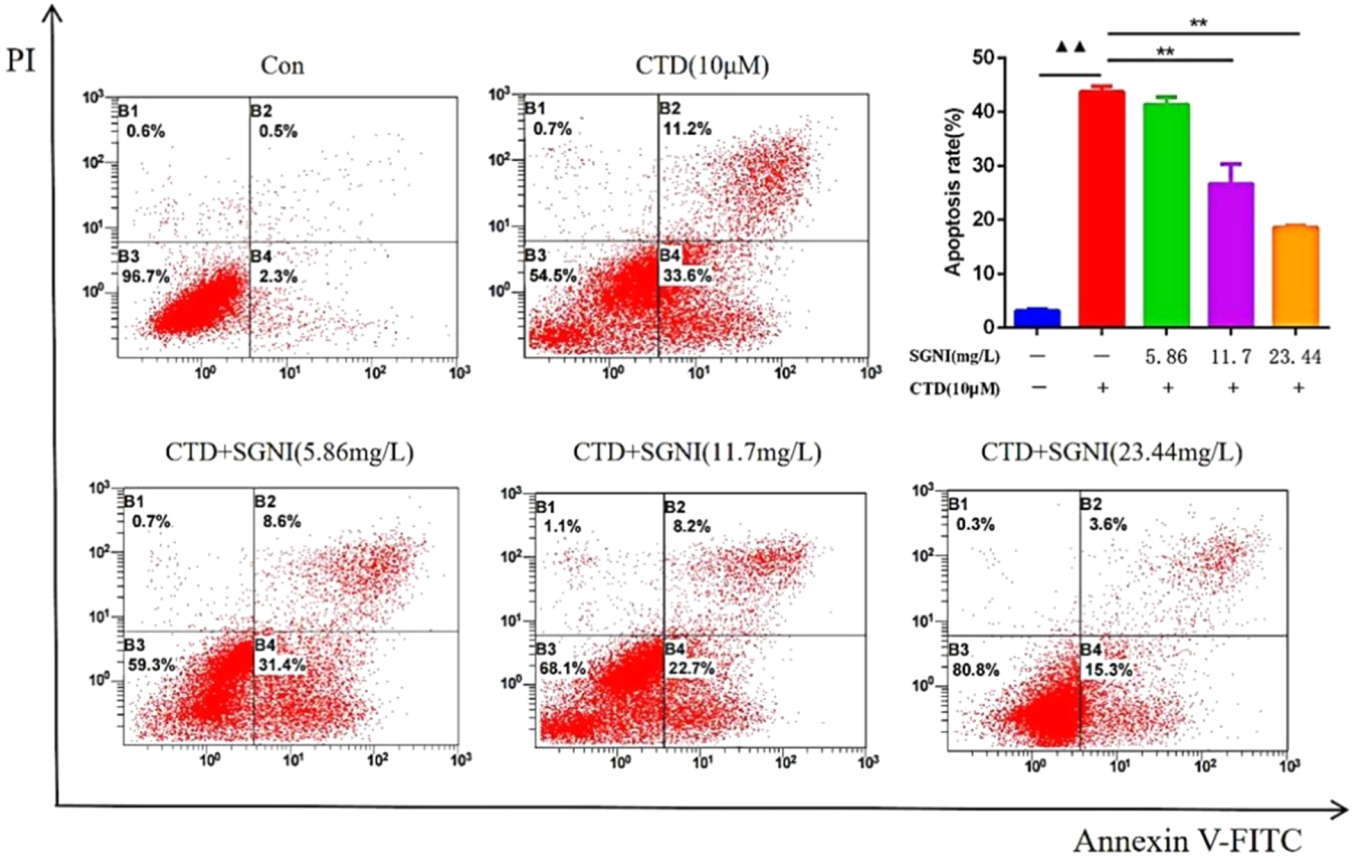

Figure 7. Antiapoptotic effects of SGNI on CTD-induced HepaRG cells. Data are expressed as mean ± SD ($n = 3$). ▲▲$p < 0.01$ compared with control, **$p < 0.01$ compared with CTD.

https://doi.org/10.1021/acsomega.3c07981
ACS Omega 2024, 9, 13692−13703

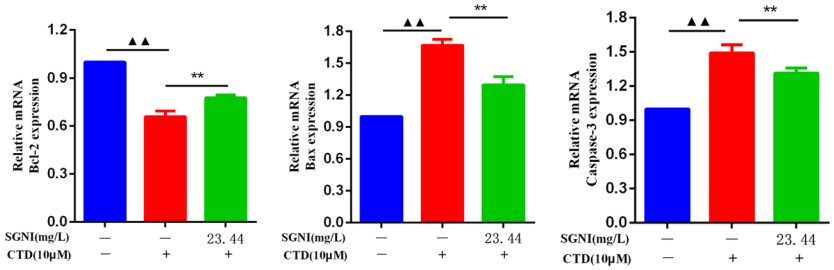

Figure 8. Effects of SGNI on the mRNA expression of Bax, Bcl-2, and Caspase-3 in CTD-induced HepaRG cells. Data are expressed as mean ± SD (n = 3). ▲▲p < 0.01 compared with control, **p < 0.01 compared with CTD.

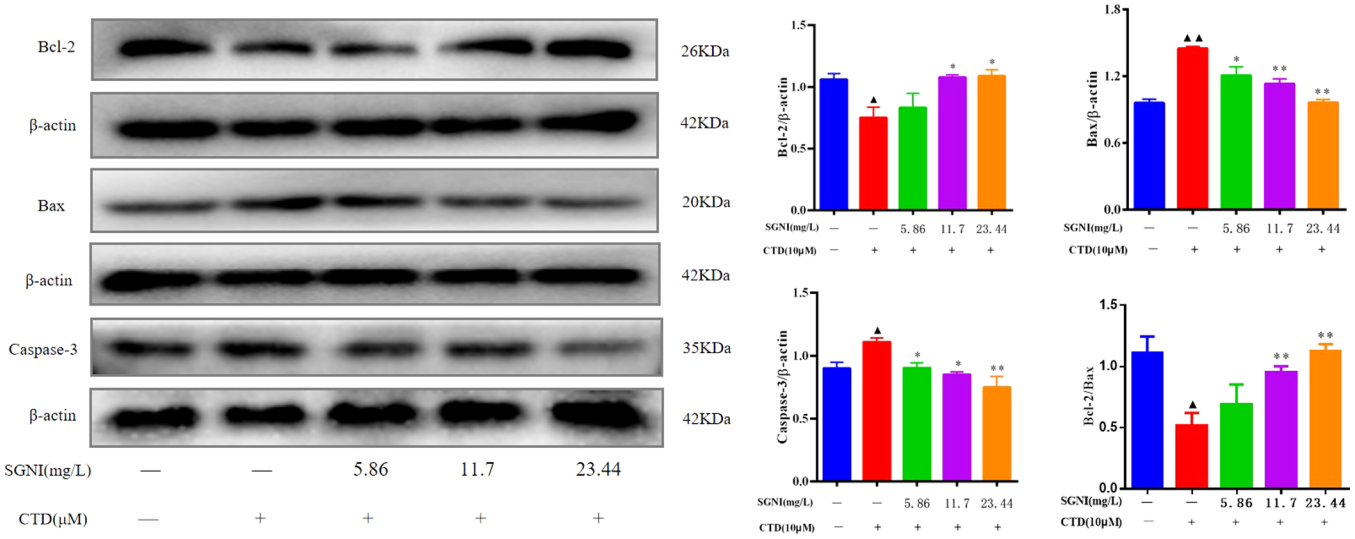

Figure 9. Expressions of apoptosis-related proteins were detected by Western blot assays. Data are expressed as mean ± SD (n = 3). ▲p < 0.05, ▲▲p < 0.01 compared with control, *p < 0.05, **p < 0.01 compared with CTD.

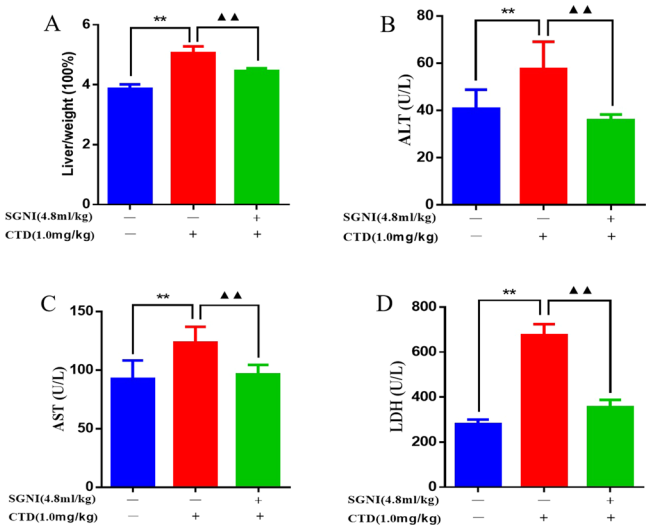

Figure 10. Liver weight/body mass and biochemical changes in control (0.5% sodium carboxymethyl cellulose solution, 1.0 mL/kg), CTD (1.0 mg/kg), and SGNI high-dose (SGNI 4.8 mL/kg+CTD 1.0 mg/kg). (A) Liver weight/body mass, (B) ALT, (C) AST, and (D) LDH.

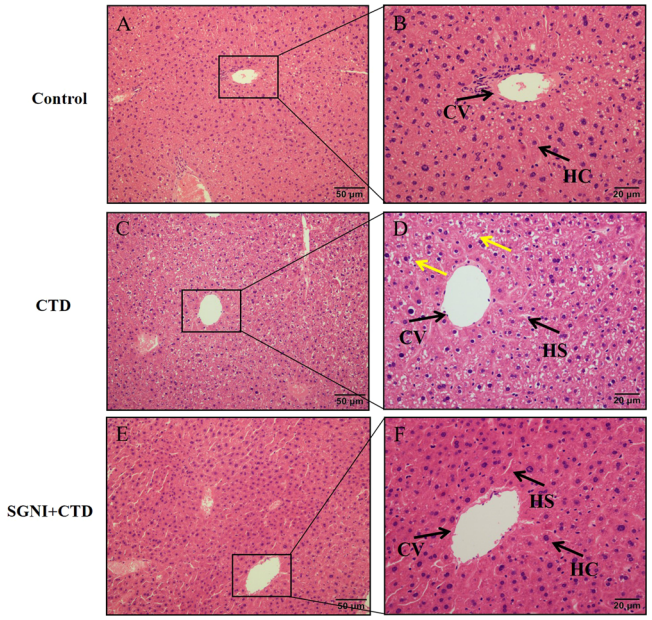

Figure 11. Histopathological changes in the mice liver: (A, B) control group; (C, D) CTD group; (E, F) SGNI+CTD group. HC: hepatocyte cords, HS: hepatic sinusoids, CV: central vein. Yellow arrow: hepatocyte steatosis and vacuole.

2.10. SGNI Pretreatment Suppressed Hepatic Apoptosis in CTD-Induced Mice. To understand the potential mechanisms of SGNI, Key proteins implicated in hepatic apoptosis were detected (Figure 12). CTD-induced mice showed increased expression of caspase-3 and Bax, whereas Bcl-2 expression decreased in the liver compared with control (p < 0.05). Compared with the CTD group, the expression levels of

https://doi.org/10.1021/acsomega.3c07981
ACS Omega 2024, 9, 13692−13703

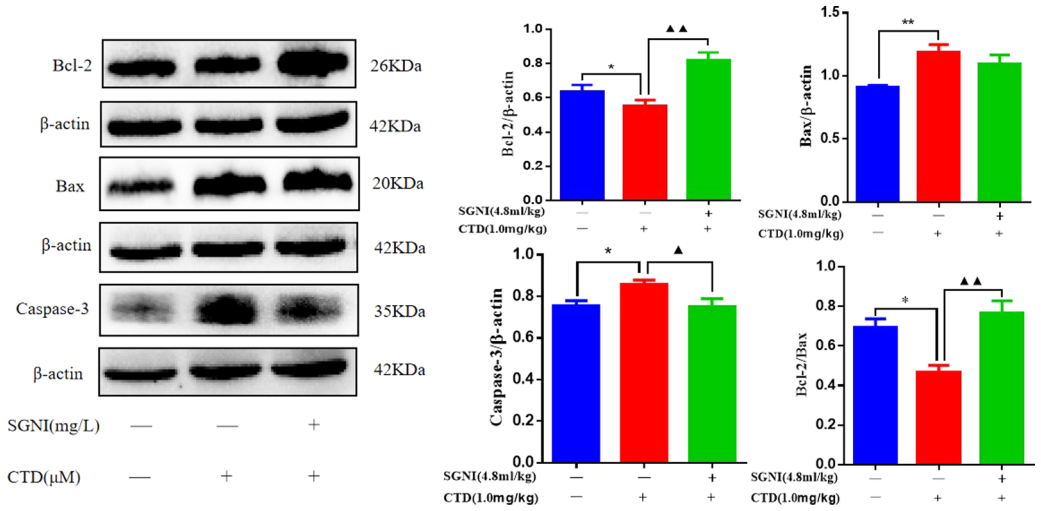

Figure 12. Expressions of apoptosis-related proteins were detected by Western blot assays. Data are expressed as mean ± SEM (n = 3). ▲p < 0.05, ▲▲p < 0.01 compared with control, *p < 0.05, **p < 0.01 compared with CTD.

caspase-3 were significantly decreased in the SGNI+CTD group, while the expression level of Bcl-2 was significantly increased (p < 0.05).

3. DISCUSSION

Modern toxicological studies have demonstrated that CTD can lead to severe liver injury when abused or overdosed, which has become the major cause of acute liver failure.[19,20] SGNI, a traditional Chinese patent medicine, has been approved by the China Food and Drug Administration (CFDA) since 2002. The medicine can treat various conditions, including clinical hepatitis, liver function impairments, fatty liver, and cholangitis. Therefore, SGNI has the potential to treat DILI. An experimental model and network pharmacology approaches were used in this study to predict and validate SGNI's therapeutic effect. According to network pharmacological analysis, SGNI was associated with liver injury, wherein cell apoptosis, oxidative stress, and inflammation were crucial to treating CTD-DILI with SGNI. Experimental results indicate that SGNI induces cell growth and inhibits cell apoptosis in vivo and that SGNI regulates the target genes of Bax, Caspase-3, and Bcl-2.

In this study, a total of 308 compounds and 438 target genes were obtained through network pharmacology. C-T network analysis identified five major ingredients: quercetin, hexacosane, hentriacontan, nonacosane, and docosanoate. Studies demonstrated that quercetin, the major active compound of SGNI, can delay the progression of DILI by suppressing cellular inflammatory response, regulating cell apoptosis, inhibiting oxidative stress, and inhibiting harmful immune responses of DILI, including cytokine-mediated proliferation, migration, and invasion.[21] These active ingredients are the primary material foundations of SGNI in CTD-DILI treatment. The Venn diagram revealed 62 core genes that were potential SGNI therapeutic targets against DILI.

To further understand the function of these genes, we conducted PPI analysis and functional enrichment analysis. After PPI topological screening with degrees, betweenness, and closeness, we discovered that hub genes, such as HSP90AA1, AKT1, MAPK1, CASP3, and JUN, may play a crucial role in the biological pathway of the SGNI treatment process. In order to determine the potential pathways of SGNI on DILI, functional enrichment analyses, including KEGG and GO analyses, were conducted. A total of 66 pathways were identified, with apoptosis, AGE-RAGE, estrogen, p53, and sphingolipid signaling pathways comprising the top five enrichment pathways. The apoptosis pathway can promote metabolism, cell proliferation, cell survival, growth, and the cell cycle by stimulating extracellular signals. Furthermore, SGNI may decrease the protein levels of Bax and Caspase-3. These results suggest that apoptosis-related pathways are crucial in SGNI's effect on DILI.

In the present study, the protective effect and action mechanism of SGNI against CTD-DILI were explored in HepaRG cells. As a result, SGNI treatment (5.86, 11.7, 23.44, 46.88 mg/L) exhibited hepatoprotective activities in response to 10 μM CTD exposure in a dose-dependent manner in HepaRG cells. AST and ALT are the most sensitive indicators of liver injury, reflecting the severity of liver cell damage, and are important indicators for evaluating hepatocyte necrosis.[22−28] Wu et al. demonstrated that *Aesculus hippocastanum* decreased the levels of ALT and AST in mice with concanavalin A-induced liver injury.[29] In our experiment, AST, ALT, and LDH expression levels increased in a concentration-dependent manner after CTD treatment and later decreased by SGNI, demonstrating that SGNI had a significant reparative effect on CTD-DILI. Furthermore, the oxidative damage index was detected in the present study. Oxidative stress, involved in the pathogenesis and progression of various liver diseases, can cause liver damage through the increased production of reactive oxygen species in response to stimulation by internal or external stimulations.[30,31] GSH-Px and SOD are antioxidant enzymes that catalyze the decomposition of hydrogen peroxide.[32] The antioxidant power of GSH-Px allows it to scavenge peroxides from living cells while protecting their membranes from the toxic effects of peroxides.[33] Free radical scavenging may be reflected in SOD activity.[34,35] MDA, an important end product of lipid peroxidation, is also a biomarker of oxidative stress.[36,37] In this study, the activities of GSH-Px and SOD in HepaRG cells decreased, whereas MDA levels increased after CTD treatment, indicating that CTD could lead to oxidative stress. These aforementioned effects were reversed with SGNI. According to these results, CTD induced oxidative stress in liver cells and SGNI reduced oxidative stress to protect liver cells against injury.

https://doi.org/10.1021/acsomega.3c07981
ACS Omega 2024, 9, 13692−13703

Multiple types of liver injury are associated with apoptosis. It is possible to reduce the incidence and mortality associated with liver failure by preventing hepatocyte apoptosis at the right moment.[38] Some studies indicated that Bcl-2 can inhibit cell apoptosis through an antioxidant way.[39,40] Overexpression of Bax can antagonize the protective effect of Bcl-2 and cause cell death by promoting cell apoptosis. To explore whether apoptosis plays a role in this study, we initially analyzed the morphology and apoptosis rates in HepaRG cells. The results demonstrated that the apoptosis rate was significantly higher in the CTD-induced cells than in the control group. However, the number of apoptotic cells decreased with the SGNI pretreatment, suggesting that SGNI has a protective effect against CTD-induced cell apoptosis. Our results validated the network analysis in which SGNI was found to inhibit the development of CTD-DILI by reducing cell apoptosis. A total of 3 core targets (apoptosis-related Bax, Bcl-2, and Caspase-3 genes) were selected for further validation. Caspase-3 is a crucial protein in the most distal effector apoptosis pathway.[41] Bcl-2 is an inhibitor gene of cell apoptosis, whereas Bax inhibits Bcl-2 and promotes cell apoptosis.[42] The qRT-PCR and Western blot results showed that SGNI could inhibit Caspase-3 and Bax expressions while decreasing the level of CTD-induced Bcl-2 protein expression, suggesting that SGNI could improve the apoptosis of CTD-induced HepaRG cells.

Given the above, we proposed a possible mechanism of SGNI against CTD-DILI (Figure 13). SGNI administration relieved

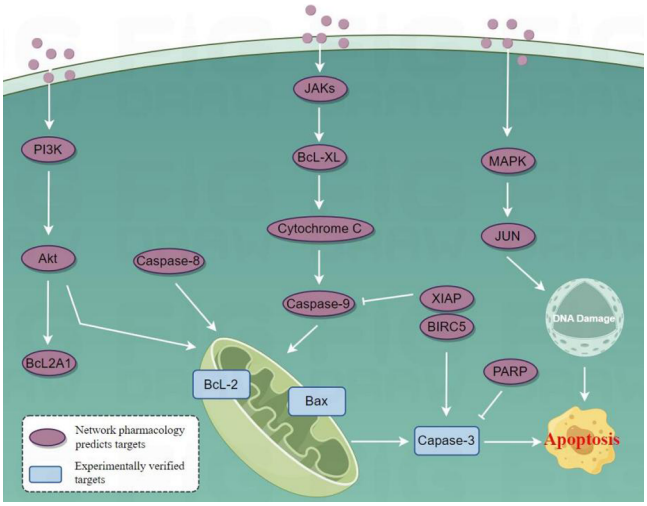

Figure 13. Proposed mechanisms of the protective effect of SGNI.

CTD-DILI by regulating the alterations of the apoptosis and oxidative stress reactions. In spite of this, our findings provide important preliminary information on SGNI's role in DILI treatment and suggest that SGNI may be a promising candidate for CTD-DILI treatment.

4. MATERIALS AND METHODS

4.1. Materials and Reagents. The human hepatocyte cell line HepaRG was obtained from the Shanghai Guandao Bioengineering Co., Ltd. (Shanghai, China). CTD (>98% purity; product batch number: 1507100; Shanghai Aladdin Biochemical Technology Co., Ltd., China). SGNI (Country Medicine Accurate Character Number: Z20025660, product batch number: 20170718) was obtained from Guizhou Ruihe Pharmaceutical Co., Ltd. (Guizhou, China) as in Figure 14A. In accordance with the National Drug Surveillance Administrative Bureau standard, the quality control standard for SGNI is that the amount of geniposide (molecular formula: $C_{17}H_{24}O_{10}$) should not be lower than 0.35 mg; the amount of baicalin (molecular formula: $C_{21}H_{18}O_{11}$) should not be lower than 18 mg when determined by HPLC. HPLC chromatogram of SGNI was performed on an Agilent ZORBAX SB-C18 (4.6 × 150 mm 5 μm). There was 0.1% phosphoric acid in water and 0.1% in acetonitrile in the mobile phases A and B. The following linear gradient was used: 0−5 min, 15%B; 5−10 min, 15−18%B; 10−15 min, 18−25%B; 15−25 min, 25%B; 25−26 min, 25−13%B; 26−30 min, 13%B. The flow rate was set to 0.8 mL/min, and the injection volume was 10 μL. The detection wavelength of baicalin and geniposide was 276 and 238 nm. HPLC chromatogram of SGNI injection is shown in Figure 14.

4.2. Active Compounds and Corresponding Target Collection. First, SGNI's chemical components were queried using TCMSP (http://tcmspw.com/tcmsp.php). Second, drug-likeness ≥0.18 and oral bioavailability ≥30% were set as screening thresholds for active compounds. Third, the genes of targets associated with "CTD" and "DILI" disease names were collected through GeneCards (https://www.genecards.org/), CTD disease database (http://ctdbase.org/), and Digsee database (http://geneSearch/). All of the network-predicted targets of SGNI liver protection were introduced into the STRING (http://string-db.org) database to conduct a PPI analysis. The hub genes were filtered by the mean degree value for the analysis. Hub genes were analyzed using DAVID 6.8 high-throughput functional annotation bioinformatics to perform functional annotation and enrichment analyses, which were then recognized with GO terms and KEGG pathways by a combined score, respectively. SGNI target-linked pathways were selected and visualized using the "Target-Pathway"network.

4.3. In Vitro Experiment Validation. *4.3.1. Cell Culture and Cell Viability Assay.* HepaRG cells were cultured in an incubator containing 5% CO_2, 100 U/mL penicillin, and 100 μg/mL streptomycin in RPMI 1640 medium. After the cells adhered completely and reached a confluence of 85%, the cells were seeded in 96-well plates at a density of 1 × 10^4 cells/well and treated with various concentrations of CTD (1.25, 2.5, 5, 10, and 20 μM) or SGNI (5.86, 11.7, 23.44, 46.88, and 93.75 mg/L) for 12 h at 37 °C. Subsequently, CCK-8 was added to the cells and incubated at 37 °C for 2 h. To determine the concentrations of CTD damage and SGNI nondamage, the OD of each well was measured at 450 nm.

To determine the protective effect of SGNI, we tested the viability of HepaRG cells with the CCK-8. The cells were treated with SGNI (5.86, 11.7, and 23.44 mg/L) for 12 h and then exposed to a CTD (10 μM) solution for another 12 h. After treating cells with 10 μL of an enhanced CCK-8 kit for 2 h, the absorbance value for each well was measured at 450 nm.

4.3.2. Effects of Liver Function and Oxidative Stress Enzyme Levels. HepaRG cells (4.0 × 10^5 cells/well) were seeded in 6-well plates for 24 h. The cells were pretreated with SGNI (5.86, 11.7, and 23.44 mg/L) for 12 h and then exposed to CTD (10 μM) for another 12 h. The cell precipitates were harvested to detect ALT, AST, LDH, SOD, GSH-Px, and MDA following the instructions of the commercial kits from Nanjing Jiancheng Bioengineering Institute (Nanjing, China).

4.3.3. Apoptosis Detected by FCS and Hoechst 33342 Staining. The cells were seeded in six-well culture plates at a density of 4 × 10^5 cells/well, cultured with SGNI (5.86, 11.7, and 23.44 mg/L) for 12 h, and then exposed to CTD (10 μM)

https://doi.org/10.1021/acsomega.3c07981
ACS Omega 2024, 9, 13692−13703

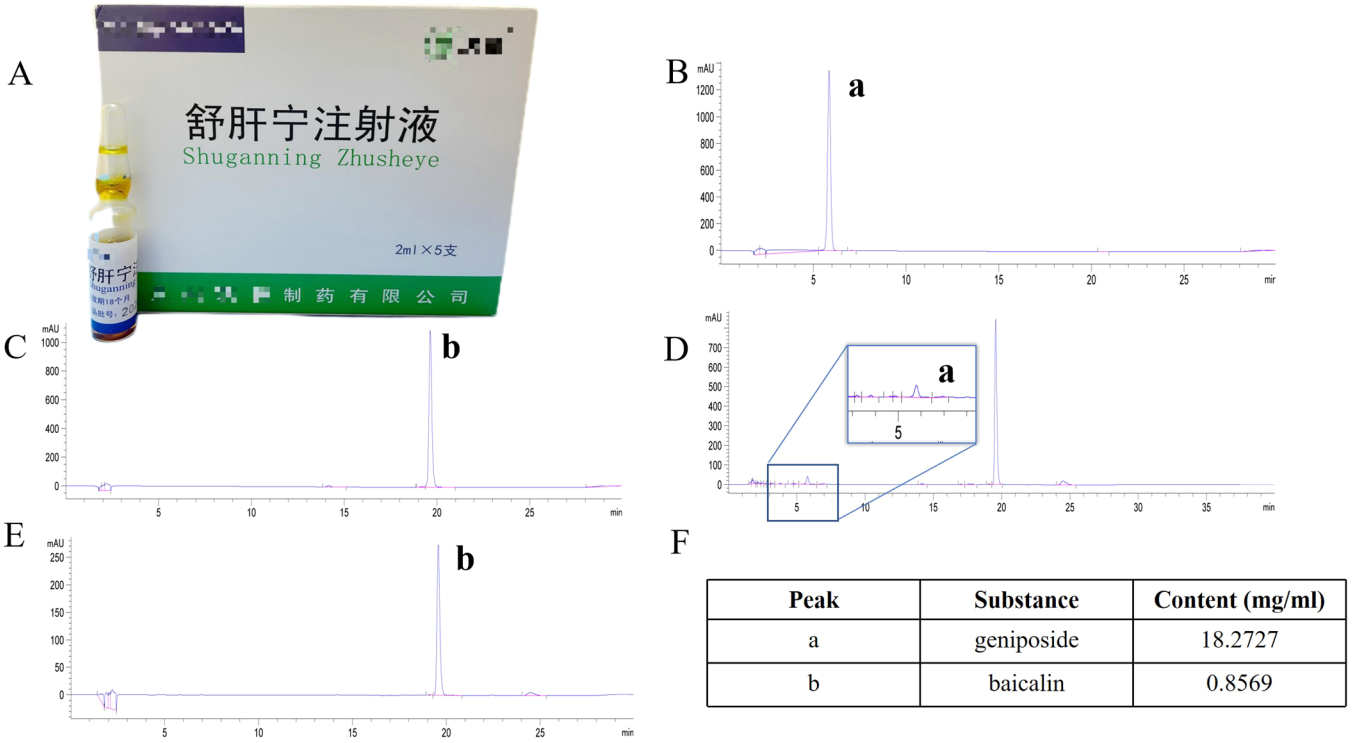

Peak	Substance	Content (mg/ml)
a	geniposide	18.2727
b	baicalin	0.8569

Figure 14. HPLC chromatogram of SGNI injection. (A) Physical picture of SGNI injection. (B) Geniposide standard. (C) Baicalin standard. (D, E) SGNI test samples (a: geniposide, b: baicalin). (F) The content determination of SGNI injection.

for another 12 h. After trypsinization, the cells were rinsed with PBS and resuspended in 400 μL of binding buffer. At room temperature, the cells were stained in darkness for 15 min with annexin V-FITC and PI. Within 1 h, the samples were analyzed by flow cytometry (Beckman Coulter, USA), and the data were analyzed using ModFit (Verity Software House, USA). Under a fluorescence microscope (Olympus Corporation, Japan), the cells were incubated with Hoechst 33342 dye to assess morphological apoptosis, and the data were analyzed using ImageJ (National Institutes of Health, USA).

4.3.4. Quantitative Real-Time PCR. Total RNA was extracted from HepaRG cells using the TRIzol reagent (cat. no. 15596-026; Thermo Fisher Scientific, Inc.) and reverse transcribed to cDNA with a Transcriptor First Strand cDNA Synthesis kit in accordance with the manufacturer's instructions. Subsequently, Light Cycler 480 SYBR Green Master Mix was used for qPCR analysis in accordance with the manufacturer's instructions. The data were analyzed by using the $2^{-\Delta\Delta Cq}$ method. The primer sequences are given in Table 3.

4.3.5. Western Blot Analysis. The cells were lysed with RIPA lysis buffer (R0010; Solarbio), and protein concentrations were then evaluated by using the BCA protein assay kit (A045-4; Nanjing Jiancheng Bioengineering Institute). Furthermore, 10 μg of proteins (HepaRG cells) or 25 μg of proteins (mice liver tissue) were separated by 12% SDS-PAGE and transferred onto PVDF membranes. In the subsequent step, the membranes were blocked with 5% fat-free dry milk for 1 h at room temperature. The blots were incubated with Caspase-3 (cat. nos. 66470; 1:2000), Bcl-2 (cat. nos. 68103; 1:5000) and Bax (cat. nos. 60267; 1:10000) (all from Proteintech, China) antibodies overnight at 4 °C. At room temperature, the membranes were incubated for 1 h with goat antirabbit IgG secondary antibodies conjugated to horseradish peroxidase (CST, 1:3000). The relative expression of each target protein was measured using β-actin as an endogenous reference.

Table 3. Primer Sequence

GeneID	primer sequence (5′−3′)	length
bax	F:CCCGAGAGGTCTTTTTCCGAG	21
	R:CCAGCCCATGATGGTTCTGAT	21
bcl-2	F:GGTGGGGTCATGTGTGTGG	19
	R:CGGTTCAGGTACTCAGTCATCC	22
caspase-3	F:GAAATTGTGGAATTGATGCGTGA	23
	R:CTACAACGATCCCCTCTGAAAAA	23
β-actin	F:AGCGAGCATCCCCCAAAGTT	20
	R:GGGCACGAAGGCTCATCATT	20

4.4. In Vivo Experiments Validation. *4.4.1. Animals and Experimental Groups.* All Sprague−Dawley mice were males aged 6 weeks, weighed 18 ± 2 g, and were obtained from the Center for Experimental Animal Research (Zunyi Medical University, China). In addition to normal diet and water ad libitum, all mice were housed under 12 h light-dark conditions. After 1 week of acclimatization, all mice were randomly divided into three groups (n = 8): control (0.5% sodium carboxymethyl cellulose solution, 1.0 mL/kg/day), CTD (1.0 mg/kg/day) and SGNI groups (SGNI 4.8 mL/kg/day+CTD 1.0 mg/kg/day). Clinical intravenous infusion of 20 mL/day for adults (60 kg) and dose for mice (4.8 mL/kg) (equivalent dose ratio table converted by body surface area between humans and animals). Before clinical use, 48% of the liquid was diluted with glucose and sodium chloride injection for use.

CTD were administered by gavage, whereas SGNI was intraperitoneal injected. The mice were treated with SGNI for 10 consecutive days, and CTD was administered every day for 7 days (Figure 15). The animal experiments were approved by the Institutional Committee on Animal Care and Use of Zunyi Medical University (SYXK 2014-003). Zunyi Medical College's

https://doi.org/10.1021/acsomega.3c07981
ACS Omega 2024, 9, 13692−13703

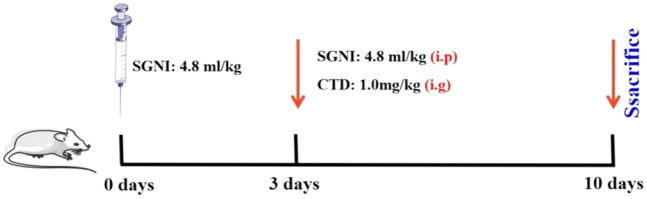

Figure 15. Hepatoprotective model construction in mice.

Institutional Animal Care and Use Committee guidelines and the National Institutes of Health Guide for the Care and Use of Laboratory Animals were followed when caring for animals and conducting experiments.

4.4.2. Measurement of Serum ALT, AST, and LDH Levels. On the 10th day of the experiment, the mice were sacrificed by cervical dislocation. At the conclusion of the treatment period, blood was collected from the orbital sinus and then centrifuged at 3000 rpm and 4 °C for 10 min to acquire the serum. The serum biochemical indices of liver function, including ALT, AST, and LDH were detected using an automatic blood biochemical analyzer (Beckman Coulter, Inc., Brea, CA, USA).

4.4.3. Histological Assessment. The livers of mice were resected and fixed in 4% paraformaldehyde, then embedded in paraffin. H&E staining was done after tissue sections had been fixed and cut into 4 cm slices. Using a light microscope equipped with a microscope camera, photomicrographs were taken (Olympus, Tokyo, Japan).

4.5. Statistical Analysis. All cellular data were expressed as mean ± SD, and animal data were expressed as mean + SEM. The data were statistically analyzed by SPSS 18.0 software. Statistical analysis was performed using a one-way analysis of variance with Tukey's multiple comparisons test for multiple comparisons. $p < 0.05$ indicated that the differences were statistically significant, and $p < 0.01$ indicated that the differences were statistically significant.

5. CONCLUSIONS

In this work, first, the possible therapeutic mechanism of SGNI on CTD-DILI was predicted by a network pharmacological approach. Second, the exact therapeutic effect of SGNI was elucidated through cell and mouse models of CTD-DILI. Finally, the mechanism of SGNI on CTD-induced apoptosis was proved by detecting the expression of bcl-2, bax, and caspase-3. The above experimental results showed that SGNI could protect the liver by preventing the CTD-induced apoptosis of hepatocytes. In conclusion, our results confirm the preventative effects of SGNI against CTD-induced hepatotoxicity by combining network pharmacological analysis and in vivo and in vitro experiment validation, making an effective paradigm for the secondary development of traditional compound formulations.

AUTHOR INFORMATION

Corresponding Authors

Xiaofei Li − *School of Basic Medicine, Zunyi Medical University, Zunyi, Guizhou 563000, China*; Phone: +86-18275608435; Email: Lixiaofei@zmu.edu.cn

Jianyong Zhang − *School of Pharmacy, Zunyi medical university, Zunyi, Guizhou 563000, China; Key Laboratory of Basic Pharmacology Ministry Education and Joint International Research Laboratory of Ethnomedicine Ministry of education, Zunyi medical University, Zunyi, Guizhou 563000, China*; Phone: +86-15120273389; Email: zhangjianyong2006@126.com

Authors

Xiaotong Duan − *School of Basic Medicine, Zunyi Medical University, Zunyi, Guizhou 563000, China*; orcid.org/0000-0002-9477-6381

Jingwen Ao − *School of Pharmacy, Zunyi medical university, Zunyi, Guizhou 563000, China*

Ming Yu − *School of Pharmacy, Zunyi medical university, Zunyi, Guizhou 563000, China*

Sali Li − *School of Basic Medicine, Zunyi Medical University, Zunyi, Guizhou 563000, China*

Complete contact information is available at: https://pubs.acs.org/10.1021/acsomega.3c07981

Author Contributions

X.D.: performed investigation, methodology, data curation, formal analysis, validation, writing-original draft. J.A., M.Y.: participated in the experimental operation and performed investigation, methodology. S.L.: participated in the experimental operation. J.Z.: conducted conceptualization, funding acquisition, project administration, formal analysis. X.L.: conducted conceptualization, funding acquisition, project administration.

Funding

This research is supported by the Guizhou Graduate Scientific Research Fund project (YJSKYJJ[2021]183); the Science and Technology Department of Zunyi City of Guizhou province of China ([2022]420, ([2020]7); the Guizhou Provincial Science and Technology Program (ZK[2022]615); the Science and technology project of Guizhou health and Health Committee ([2021]441); Guizhou Provincial Special Research Project on Science and Technology of Traditional Chinese Medicine and Ethnic Medicine ([2021]035); Guizhou Provincial Department of Health Outstanding Young Medical Talents Fund ([2021]3); Guizhou Province Youth Science and Technology Talent Plan (YQK[2023]038).

Notes

The authors declare no competing financial interest.

REFERENCES

(1) Feng, S.; Zhu, J.; Xia, K.; et al. Cantharidin Inhibits Anti-Apoptotic Bcl-2 Family Proteins and Induces Apoptosis in Human Osteosarcoma Cell Lines MG-63 and MNNG/HOS via Mitochondria-Dependent Pathway. *Med. Sci. Monit* **2018**, *24*, 6742−6749.

(2) Hsia, T. C.; Yu, C. C.; Hsu, S. C.; et al. cDNA microarray analysis of the effect of cantharidin on DNA damage, cell cycle and apoptosis-associated gene expression in NCI-H460 human lung cancer cells in vitro. *Molecular Medicine Reports* **2015**, *12* (1), 1030−1042.

(3) Zhang, C.; Chen, Z.; Zhou, X.; et al. Cantharidin induces G2/M phase arrest and apoptosis in human gastric cancer SGC-7901 and BGC-823 cells. *Oncol Lett.* **2014**, *8* (6), 2721−2726.

(4) Shen, M.; Wu, M. Y.; Chen, L. P.; et al. Cantharidin represses invasion of pancreatic cancer cells through accelerated degradation of MMP2 mRNA. *Sci. Rep.* **2015**, *5*, No. 11836.

(5) Li, W.; Xie, L.; Chen, Z.; et al. Cantharidin, a potent and selective PP2A inhibitor, induces an oxidative stress-independent growth inhibition of pancreatic cancer cells through G2/M cell-cycle arrest and apoptosis. *Cancer Sci.* **2010**, *101* (5), 1226−33.

(6) Yu, M.; Zhao, Y. Cantharis by photosynthetic bacteria biotransformation: Reduced toxicity and improved antitumor efficacy. *J. Ethnopharmacol* **2016**, *186*, 151−158.

https://doi.org/10.1021/acsomega.3c07981
ACS Omega 2024, 9, 13692−13703

(7) Liu, F.; Duan, C.; Zhang, J.; et al. Cantharidin-induced LO2 cell autophagy and apoptosis via endoplasmic reticulum stress pathway in vitro. *J. Appl. Toxicol* **2020**, *40* (12), 1622−1635.
(8) Moye, V. A.; Cathcart, S.; Morrell, D. S. Safety of cantharidin: a retrospective review of cantharidin treatment in 405 children with molluscum contagiosum. *Pediatr Dermatol* **2014**, *31* (4), 450−4.
(9) Wu, W.; Su, M.; Li, T.; et al. Cantharidin-induced liver injuries in mice and the protective effect of vitamin C supplementation. *Int. Immunopharmacol* **2015**, *28* (1), 182−7.
(10) Lao, X. N. Therapeutic effect of Shugan Decoction on drug-induced hepatitis. *Tradit. Chinese Med. Mater.* **2004**, No. 06, 467−468.
(11) Liang, H. X.; et al. Clinical study of Shuganing Injection in the treatment of chronic viral hepatitis B: Meta-analysis. *World J. Integrat. Chinese Western Med.* **2016**, *11* (08), 1057−1062. +1066
(12) Zhang, Q.; et al. Effects of Shuganing Injection on liver function and bilirubin in patients with chronic viral hepatitis B hyperbilirubinemia. *Chin. Med. Guide* **2014**, *20* (16), 71−73.
(13) Wang, Y. C.; Wang, J. Q. Research progress in clinical application of Shuganing Injection. *Chinese Pharmacovigil.* **2020**, *17* (8), 543−548.
(14) Bian, H. Z. Study on improving effect of Shuganing Injection on ascites of liver cirrhosis in rats. *Chinese Pharm.* **2012**, *23* (19), 1740−1741.
(15) Jin, Z. Protective effect of Shuganing Injection on liver injury in mice poisoned by cisplatin. *Chinese Pharm.* **2016**, *27* (7), 920−922.
(16) Zhao, L.; et al. Protective effect of Shuganing Injection on experimental liver injury in mice. *Pharmacol. Clin. Chinese Med.* **2007**, *6*, 65−67.
(17) Susilo, R. J. K.; Winarni, D.; Husen, S. A.; et al. Hepatoprotective effect of crude polysaccharides extracted from Ganoderma lucidum against carbon tetrachloride-induced liver injury in mice. *Vet World* **2019**, *12* (12), 1987−1991.
(18) Tang, F.; Tang, Q.; Tian, Y.; et al. Network pharmacology-based prediction of the active ingredients and potential targets of Mahuang Fuzi Xixin decoction for application to allergic rhinitis. *J. Ethnopharmacol* **2015**, *176*, 402−12.
(19) Zhang, J. Q.; et al. Advances in toxicology of cantharidin compounds. *China Pharmacist* **2019**, *22* (08), 1503−1506.
(20) Zhu, S. S.; Long, R.; Song, T.; et al. UPLC-Q-TOF/MS Based Metabolomics Approach to Study the Hepatotoxicity of Cantharidin on Mice. *Chem. Res. Toxicol.* **2019**, *32* (11), 2204−2213.
(21) Chen, T.; Zhang, X.; Zhu, G.; et al. Quercetin inhibits TNF-α induced HUVECs apoptosis and inflammation via downregulating NF-kB and AP-1 signaling pathway in vitro. *Medicine (Baltimore)* **2020**, *99* (38), No. e22241.
(22) McGill, M. R. The past and present of serum aminotransferases and the future of liver injury biomarkers. *EXCLI J.* **2016**, *15*, 817−828.
(23) Hanley, A. J.; Williams, K.; Festa, A.; et al. Elevations in markers of liver injury and risk of type 2 diabetes: the insulin resistance atherosclerosis study. *Diabetes* **2004**, *53* (10), 2623−32.
(24) Uchida, N. S.; Silva-Filho, S. E.; Cardia, G. F. E.; et al. Hepatoprotective Effect of Citral on Acetaminophen-Induced Liver Toxicity in Mice. *Evid. Based Complement. Alternat. Med.* **2017**, *2017*, No. 1796209.
(25) Zhang, L. J. Determination of serum transaminase and its clinical significance. *Chinese Med. Guide* **2012**, *10* (9), 298−299.
(26) Wang, Y.; Tang, C.; Zhang, H. Hepatoprotective effects of kaempferol 3-O-rutinoside and kaempferol 3-O-glucoside from Carthamus tinctorius L. on CCl(4)-induced oxidative liver injury in mice. *J. Food Drug Anal* **2015**, *23* (2), 310−317.
(27) Lehmann-Werman, R.; Magenheim, J.; Moss, J.; et al. Monitoring liver damage using hepatocyte-specific methylation markers in cell-free circulating DNA. *JCI Insight* **2018**, *3* (12), No. e120687, DOI: 10.1172/jci.insight.120687.
(28) Wang, G. W.; Zhang, X. L.; Wu, Q. H.; et al. The hepatoprotective effects of Sedum sarmentosum extract and its isolated major constituent through Nrf2 activation and NF-κB inhibition. *Phytomedicine* **2019**, *53*, 263−273.
(29) Wu, S.; Sa, R.; Gu, Z.; et al. The Protective Effect of Aesculus hippocastanum (Venoplant®) Against Concanavalin A-Induced Liver Injury. *Pharmacology* **2019**, *104* (3−4), 196−206.
(30) Li, S.; Hong, M.; Tan, H. Y.; et al. Insights into the Role and Interdependence of Oxidative Stress and Inflammation in Liver Diseases. *Oxid. Med. Cell. Longevity* **2016**, *2016*, No. 4234061.
(31) Xu, N.; Gao, Z.; Zhang, J.; et al. Hepatoprotection of enzymatic-extractable mycelia zinc polysaccharides by Pleurotus eryngii var. tuoliensis. *Carbohydr. Polym.* **2017**, *157*, 196−206.
(32) García-Niño, W. R.; Zatarain-Barrón, Z. L.; Hernández-Pando, R.; et al. Oxidative Stress Markers and Histological Analysis in Diverse Organs from Rats Treated with a Hepatotoxic Dose of Cr(VI): Effect of Curcumin. *Biol. Trace Elem Res.* **2015**, *167* (1), 130−45.
(33) Pompella, A.; Corti, A. Editorial: the changing faces of glutathione, a cellular protagonist. *Front. Pharmacol.* **2015**, *6*, No. 98.
(34) Gao, Y.; Tang, H.; Xiong, L.; et al. Protective Effects of Aqueous Extracts of Flos lonicerae Japonicae against Hydroquinone-Induced Toxicity in Hepatic L02 Cells. *Oxid. Med. Cell Longevity* **2018**, *2018*, No. 4528581.
(35) Nojima, Y.; Ito, K.; Ono, H.; et al. Superoxide Dismutases, SOD1 and SOD2, Play a Distinct Role in the Fat Body during Pupation in Silkworm Bombyx mori. *PLoS One* **2015**, *10* (2), No. e0116007, DOI: 10.1371/journal.pone.0116007.
(36) Busch, C. J.; Hendrikx, T.; Weismann, D.; et al. Malondialdehyde epitopes are sterile mediators of hepatic inflammation in hypercholesterolemic mice. *Hepatology* **2017**, *65* (4), 1181−1195.
(37) Li, S.; Tan, H. Y.; Wang, N.; et al. The Role of Oxidative Stress and Antioxidants in Liver Diseases. *Int. J. Mol. Sci.* **2015**, *16* (11), 26087−124.
(38) Luedde, T.; Kaplowitz, N.; Schwabe, R. F. Cell death and cell death responses in liver disease: mechanisms and clinical relevance. *Gastroenterology* **2014**, *147* (4), 765−783.
(39) Petit, A.; Mwale, F.; Zukor, D. J.; et al. Effect of cobalt and chromium ions on bcl-2, bax, caspase-3, and caspase-8 expression in human U937 macrophages. *Biomaterials* **2004**, *25* (11), 2013−8.
(40) Man, N.; Tan, Y.; Sun, X. J.; et al. Caspase-3 controls AML1-ETO-driven leukemogenesis via autophagy modulation in a ULK1-dependent manner. *Blood* **2017**, *129* (20), 2782−2792.
(41) Kalkavan, H.; Green, D. R. MOMP, cell suicide as a BCL-2 family business. *Cell Death Differ.* **2018**, *25* (1), 46−55.
(42) Franklin, J. L. Redox regulation of the intrinsic pathway in neuronal apoptosis. *Antioxid Redox Signal* **2011**, *14* (8), 1437−48.

https://doi.org/10.1021/acsomega.3c07981
ACS Omega 2024, 9, 13692−13703